1. Introduction

A concrete-filled tube (CFT) column consists of a steel tube filled with concrete. The concrete core adds stiffness and compressive strength to the tubular column and reduces the potential for inward local buckling. Conversely, the steel tube acts as longitudinal and lateral reinforcement for the concrete core helping it to resist tension, bending moment and shear and providing confinement for the concrete. Due to the benefit of composite action of the two materials, the CFT columns provide excellent seismic event resistant structural properties such as high strength, high ductility and large energy absorption capacity. Also, circular hollow sections possess many advantages over open sections, including aesthetic appearance and economy in terms of material costs. Due to the complexity of connections between steel beams and circular hollow sections, their use in structural steelwork is limited. This is because the use of standard bolting is not feasible and costly unpopular welded connections are the normal solution. The numerous failures of fully welded moment connections during the 1994 Northridge and 1995 Kobe earthquakes indicated that conventional fully welded moment connections had several inherent drawbacks, whereas bolted and riveted connections had performed well in past earthquakes, particularly when encased in concrete (Swanson and Leon, 2000). An innovative beam-to-CFT column connection using blind bolts has been developed for loading conditions at regions of low to medium seismicity.

2. Experimental program

A series of tests on blind-bolted T-stub connection were conducted at the University of Melbourne to study the structural behaviour of this type of connection (Gardner and Goldsworthy 2005). A typical test specimen is shown in Figure 1, which represents an exterior column segment. The specimen consisted of a concrete-filled steel tube, a curved endplate, and a flared flange plate. The curved endplate of the T-stub was fastened to the circular tube by Ajax blind bolts with or without extensions into the concrete of the column. The tensile behaviour of the T-stub element is critical to the seismic performance of the beam-column connection.

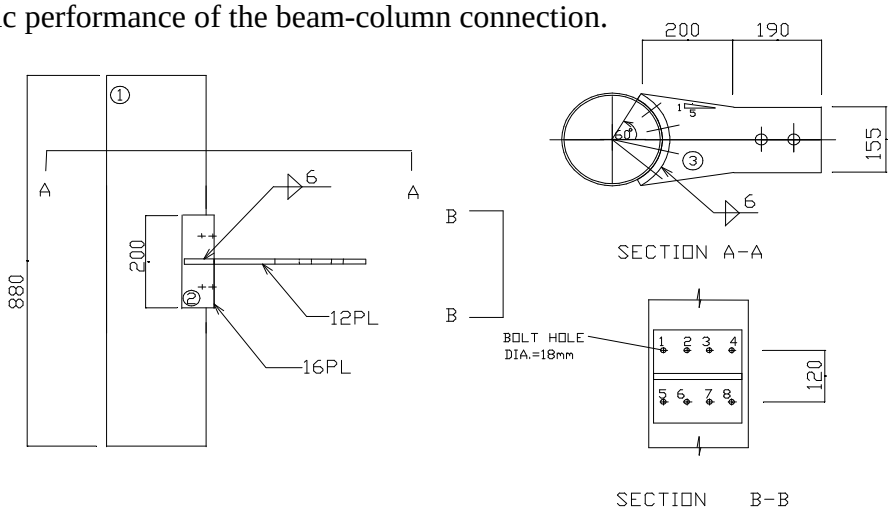

① 219.1dia. × 4.8 CHS L=880mm
② END PLATE 200 × 230mm t=16mm
③ WEB PLATE

Figure 1 Test specimen

The tube was a 219.1x4.8mm circular hollow section of grade 350, which was approximately two thirds of the size of a prototype column. The 16mm thick plate of grade 300 was curved as an endplate by brake pressing. The flared flange was fabricated from grade 250 plate and shop welded to the endplate. The 12mm diameter Ajax blind bolts had a minimum tensile strength of 800MPa and yield strength of 640MPa. The extensions welded to the head of the bolts were 12mm diameter reinforcing bars of grade 400MPa. Figure 2 shows specimen 1 without any extension to the blind bolts, whereas Figure 3 shows specimen 3 with cogged bar extensions attached to the blind bolts. The tubes were filled with concrete of 30MPa characteristic compressive strength.

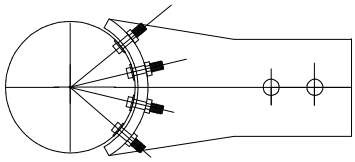

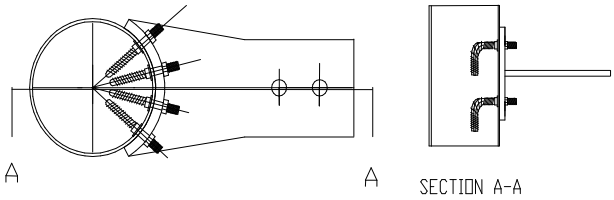

Figure 2 Blind bolts without extension **Figure 3** Blind bolts with extensions

Each specimen was fixed to laboratory strong floor with reaction frame. A hydraulic actuator of 500KN capacity was used to apply tension load to the flared flange plate through a loading plate. Four LVDTs were installed on the flange so as to measure any displacement of the endplate relative to the concrete-filled steel tube.

3. Numerical modelling

In the field of structural engineering, results from finite element simulation may provide detailed information on the stress and the strain distributions in structures. Such information is not easily available from experiments, and, therefore, numerical investigation may be used to provide supplementary data for improved understanding. Furthermore, parametric studies on the finite element models may be performed to improve the efficiency of structural design. In recent years, advancement in finite element formulation has produced robust algorithms in handing large deformation, plasticity and contact compatibility. ANSYS, version 8.1, a large-scale general purpose finite element code was selected for this analysis.

3.1 Description of model

An overall model of the T-stub connection to the CFT column is shown in Figure 4. Due to symmetry, only a quarter of the specimen was analysed. Symmetric boundary conditions were imposed on the two symmetric planes, one longitudinal plane along central line and one transverse plane at middle height of the tube and the endplate. Thus, a quarter model was used in the detailed FE study (see Figure 5).

In the three-dimensional model, eight-node iso-parametric solid elements SOLID45 were employed to model the circular hollow section, curved endplate, flange plate, round headed bolts, nuts and split washers. The mesh pattern of the curved endplate and flared flange plate is shown in Figure 6. The cogged bar extensions to the blind bolts were simulated by the non-linear spring element COMBIN39, which represented the

interaction between the reinforcing bar and the surrounding concrete within a confined environment. The behaviour of the anchorage of springs was obtained through an analytical algorithm, which had been validated by an extensive experimental program (Yao et al. 2004). The springs were attached to the bolt head using a multi-point constrain approach with a pilot node. The configuration of solid elements representing the bolts, and spring elements representing the associated extensions is shown in Figure 7.

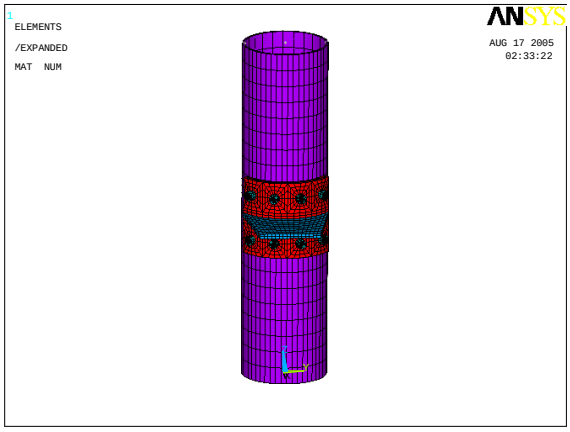

Figure 4 Overall model

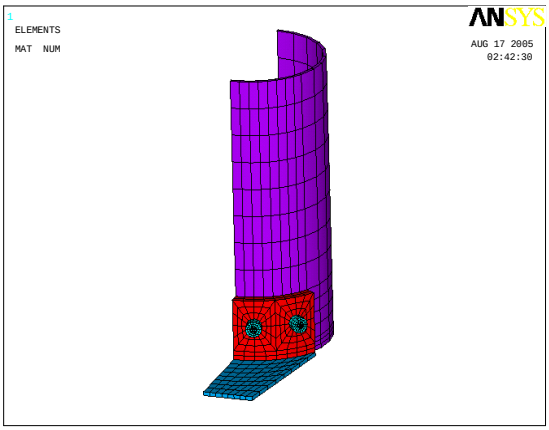

Figure 5 Quarter model

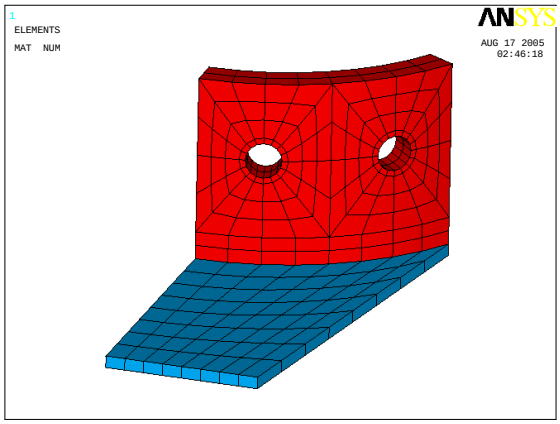

Figure 6 Endplate and flange

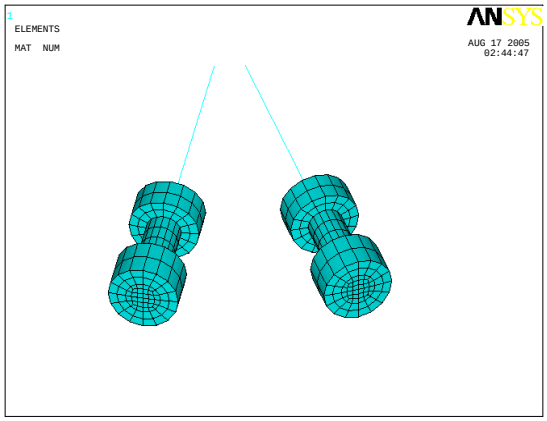

Figure 7 Bolts and extensions

The concrete core was idealized as a rigid body so as to reduce the number of solid elements. The complex interaction between the surfaces of the concrete core and steel tube, curved endplate and steel tube, bolt head/washer with steel tube, nut/washer with endplate, and bolt shank and endplate were modelled with surface-to-surface contact and target elements (TARGET169 and CONTA174). These contact elements were overlaid on the parts of the model that were analysed for interaction. The surface-to-surface contact elements had several advantages over node-to-node elements, including that they supported surface discontinuities, large sliding and deformations. Since the bolt head and nut stayed in close contact with their connecting components through all load steps, they were defined as continuous with both the tube wall and the endplate nodes respectively in order to reduce the number of contact pairs in this region. The bolt,

washer and nut were considered as one unit to limit the number of contact elements in the model.

3.2 Material properties

The material behaviour of the steel tube, endplate, flange, bolt and washer were described by bilinear stress-strain curves as shown in Figure 8. The initial slope of the curve was taken as the elastic modulus, E_0, of the material and the post yield stiffness identified as the tangent modulus, E_1, was taken as 10% of the initial stiffness ($E_1=0.1E_0$). Plasticity-based isotropic hardening using the von Mises yield criterion was employed to obtain the response of the connection in the inelastic region. The typical behaviour of the anchorage spring is shown in Figure 9.

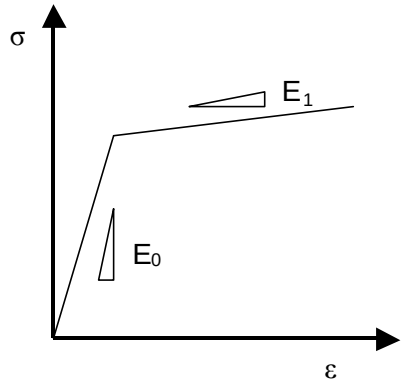

Figure 8 Idealized material behaviour

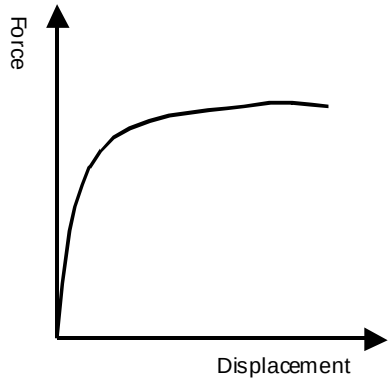

Figure 9 Nonlinear spring behaviour

3.3 Loading and boundary conditions

Nonlinearity in the behaviour of the blind-bolted T-stub connection was ascribed mainly to material plasticity and partially to changes in the contact areas among endplate, tube wall, blind bolt and nuts. Therefore, this required that, in addition to multiple iterations per load step for convergence, the loads be applied gradually, in increments, to characterize the actual load history. Symmetric displacement boundary conditions were defined for the nodes along the two planes of symmetry.

3.4 Modelling procedure

Specimen 1 and specimen 3 were selected for finite element analysis. In specimen 1, the curved endplate was fastened to the CFT column with blind bolts only, whereas additional cogged bar extensions were provided to the end of the blind bolts for specimen 3. The identical load and load steps were applied to the end of the flared flange plate in tension. The top and bottom surface elements of the CFT column were fixed to simulate the testing conditions in which the reaction frame held the column in position.

Both of the specimens were analysed in two scenarios based on different clamping action between the endplate and the tube wall. In the first case, the curved endplate was assumed to be fully clamped with the steel tube wall by applying the full pretension

load to the bolts. A bonded always algorithm was introduced to the target and contact pairs between the endplate and the tube wall. An initial stiffness could be obtained in this FE analysis. In the second case, the endplate was fastened to the tube wall in snug tight condition. A normal contact was set up between the endplate and tube wall to simulate that situation.

In the experimental program, the blind bolts were pretensioned to 48.9KN (65% of the proof load) with a torque wrench. Therefore, the designated scenarios will be upper and lower bounds for the testing specimens.

4. Analytical results

4.1 Specimen 1

This specimen had no cogged extensions affixed to the blind bolts. The total tension load was applied to the flange plate in twelve sub steps. Load versus endplate displacement was recorded, where the endplate displacement is the relative movement in the direction of the load between the endplate and the tube wall. At 220KN, the endplate moved 0.524mm and the maximum displacement was 6.9mm at the load of 380KN. Figure 10 and 11 show the displacement of endplate and the von Mises stress distribution on the endplate and adjacent area on the tube wall at the load of 380KN. Tension on the bolts caused the tube wall to bubble outwards around each bolt. The tube wall suffered from the localised bearing from the washers and the material around each hole deformed plastically. Consistent with this, in the test program the tube fractured close to some of the bolts and they eventually pulled through the tube. The theoretically predicted plastic deformation of the bolts themselves is shown in Figure 12.

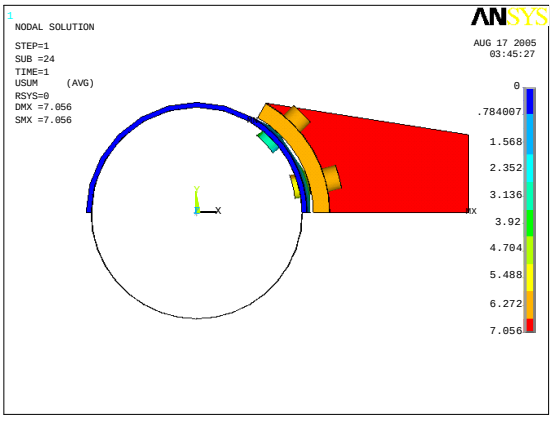

Figure 10 Displacement of specimen 1

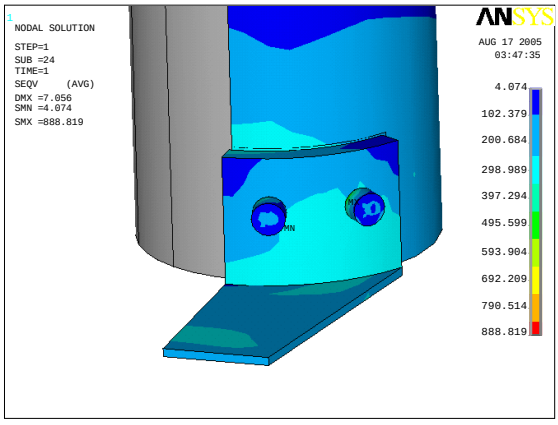

Figure 11 Von Mises stress of specimen 1

The comparison between test result and FE model result is shown in Figure 13. The FE model of the first case represents the initial stiffness of the T-stub connection well. The second case, using the snug-tight condition, was more flexible at the beginning stage compared to the test result, which had partial preload on the bolts. After the pretension on the bolts was released, the behaviour of the two curves was quite similar.

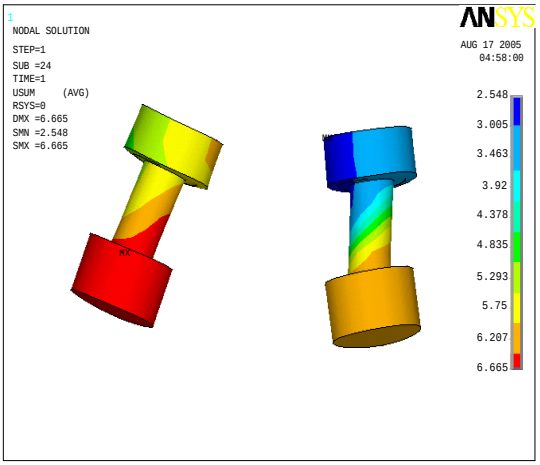

Figure 12 Deformation of bolts in specimen1

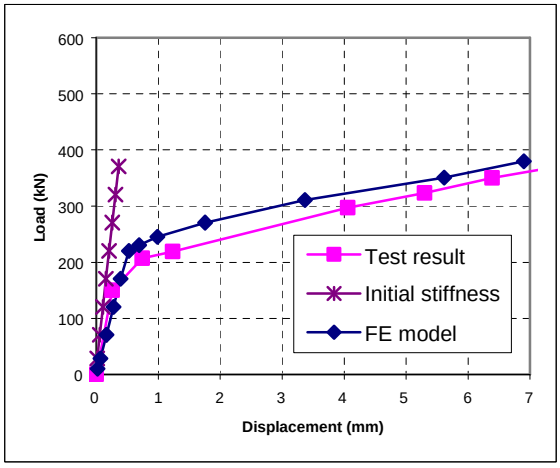

Figure 13 Load-displacement of specimen 1

4.2 Specimen 3

Specimen 3 had cogged bar extensions attached to the bolt heads. In the tests, a few bolts suffered a fracture in the weld connecting the bolts to the extensions. In the model, this would not occur as the extension was idealized as a spring attached to the pilot node of the bolt head. At load of 220KN, 370KN and 500KN, the middle line of the endplate had displacement of 0.417mm, 0.961mm and 3.637mm respectively. Figure 14 and 15 show the displacement of the endplate and the von Mises stress distribution on the endplate and on the tube wall at the load of 500KN. Due to the benefit of the anchorage of the cogged bar extension within the concrete, the displacement was reduced and a higher load could be achieved. Figure 16 demonstrates less deformation and movement of the bolts. The comparison of results of FE modelling and experimental test is shown in Figure 17. The numerical results were found to be in good agreement with the actual performance in the test.

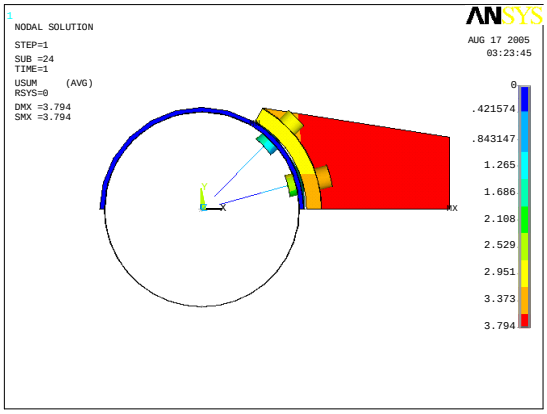

Figure 14 Displacement of specimen 3

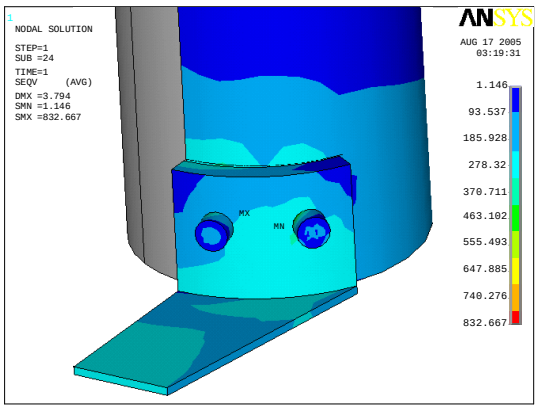

Figure 15 Von Mises stress of specimen 3

The differences between numerical and experimental curves can have a variety of sources, often being a direct consequence of the simplifications introduced in the numerical modelling. Among these factors are (i) imperfections originated from the

assembly of the tested models; (ii) the effects of residual stresses; and (iii) representation of stress-strain behaviour for materials in the FE models.

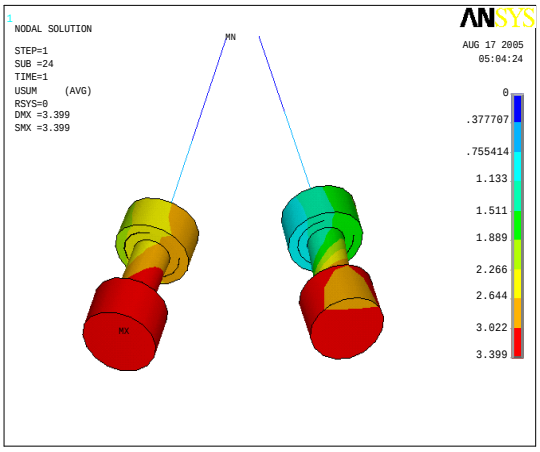

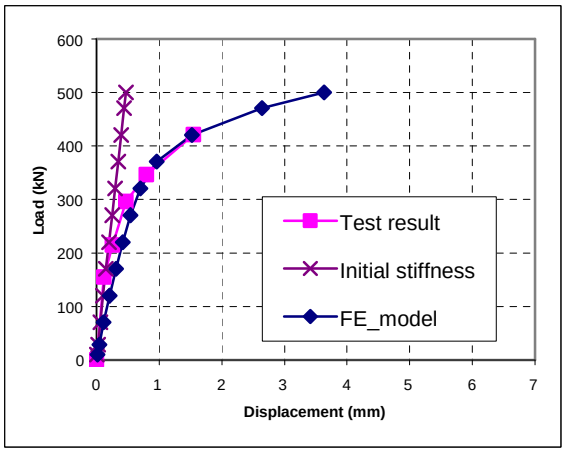

Figure 16 Deformation of bolts and extensions **Figure 17** Load-displacement of Specimen 3

4.3 Discussion on bolt pretension

The effect of pretensioning the bolts is to increase the stiffness of a connection at levels below the ultimate. Pretensioning has little effect, if any, on the strength of a connection. The result of bolt pretension in the connection is to delay the contribution of bolts to the deformation and rotation by introducing contact pressure between the plies. In other words, snug-tight bolts simply allow the plates to pull away and change their curvature at low levels of load. Nonetheless, as the contact pressure due to bolt pretension is relieved and or shifted to other parts of the plate, the deformation of the connection tends to follow the same pattern as its snug-tight counterpart. In connections with thick endplates, the influence of pretensioning of the bolts on their early stiffness is more than for a thin endplate as the latter obtains most of its deformability from the bending of the endplate rather than bolt extension. The effects of bolt pretenion on the connection behaviour will be the subject of a separate investigation, which is part of the comprehensive research program.

5. Conclusions

A 3D finite element model incorporating contact and nonlinear material properties can be employed to study numerically the stiffness and deformation of the blind-bolted T-stub connection as part of a comprehensive research program to investigate the behaviour of the moment-resisting beam-to-CFT column connection. The numerical results were found to be in good qualitative agreement with the actual connection behaviour, although they also revealed remaining difficulties in quantifying the clamping effects on the connection due to the pretension in the bolts. The T-stub connection to CFT column using blind bolts and extensions involve complex phenomena, clearly hard to simulate with simplified analytical formulations. The developed FE model can be used as a potential tool for parametric studies in order to improve the characterization of the actual behaviour of the connections.

Acknowledgements

The authors are grateful for the support provided by Civil and Environmental Engineering Department for the contribution to the license of the finite element software package.

References

1. ANSYS Element Reference, ANSYS 8.1 documentation. Online help.

2. Gardner A. P. and Goldsworthy H. M. (2005). “Experimental investigation of the stiffness of critical components in a moment-resisting composite connection”, Journal of Constructional Steel Research, Vol. 61, p709-726.

3. Swanson J. A. and Leon R. T. (2000). “Bolted steel connections: tests on T-stub components”, Journal of Structural Engineering, ASCE, Vol. 126, No.1.

4. Yao H., Goldsworthy H. M., and Gad E. F, (2004). "Anchorage of critical elements in a moment-resisting steel I beam-to-CFT column connection", Proceedings of the 2004 Conference of the Australian Earthquake Engineering Society, Mt. Gambier, paper no.7.